Iranian Journal of Hydrogen & Fuel Cell 2(2021) 95-101

Iranian Journal of Hydrogen & Fuel Cell

IJHFC

Journal homepage://ijhfc.irost.ir

Kinetics study of hydrogen evolution reaction on a high porous three dimensional NiPC alloy

Ramin Badrnezhad[a], Samaneh Asadi[b], Ali Reza Madram[a,*]

[a] Department of Chemistry and Chemical Engineering, Malek-Ashtar University of Technology, Tehran, 15875-1774 Iran.
[b] Seyyed Jamaleddin Asadabadi University, Asadabad, 6541861841, Iran.

Article Information

Article History:

Received:
05 Mar 2021
Received in revised form:
21 Jul 2021
Accepted:
09 Aug 2021

Keywords

Hydrogen evolution reaction (HER)
Three-dimensional NiPC alloy
Electrocatalytic activity
Electrodeposition

A high porous three-dimensional structure of ternary NiPC alloy (3D-NiPC) was prepared with a simple, cheap, and efficient method called dynamic hydrogen bubble template (DHBT) and characterized by means of microstructural and electrochemical techniques with regard to its catalytic effect toward the hydrogen evolution reaction (HER) in an alkaline solution. The electrochemical efficiency of the alloy has been evaluated on the basis of electrochemical data obtained from the steady-state polarization Tafel curves and electrochemical impedance spectroscopy (EIS) in a 1 M NaOH solution at 298 K. The results showed that the three-dimensional structure of NiPC alloy effectively increased its catalytic activity toward the HER. The 3D-NiPC alloy is characterized by low overpotential at practical high current densities, large real surface area, and double-layer capacitance. Also, the 3D-NiPC showed very good physical and electrochemical stability. A high roughness factor (three orders of magnitude; R_f=3550), low overpotential at 250 mAcm^{-2} (η_{250}=173.3 mV), and low charge transfer resistance (R_{ct}=100 Ωcm^2) were obtained in the best conditions, in 1 M NaOH at 298 K.

1. Introduction

With the ever-increasing use of fossil fuels in recent decades and the resulting release of millions of tons of carbon dioxide into the atmosphere, global warming has become a serious issue. Hydrogen gas is considered to be a promising alternative candidate for fossil fuels, mainly due to its regenerative and nonpolluting features. In addition, hydrogen as an energy carrier can be widely used in different areas, noticeably in fuel cells. One of the most important methods to

*Corresponding author: ar.madram@gmail.com

doi: 10.22104/IJHFC.2021.4767.1218

produce clean hydrogen is water electrolysis, which consists of two half reactions: oxygen (O_2) evolution reaction (OER) and hydrogen (H_2) evolution reaction (HER) [1]. The HER in aqueous solution is one of the most studied electrode reactions because of its importance in both fundamental and technological electrochemistry. Many types of catalysts have been investigated for HER [2-8]. The most studied cathodic material for HER is Ni and its alloys [9,10]. Therefore, various Ni-based catalysts, such as NiCo, NiZn, NiP, NiS, etc., have been synthesized and their HER evaluated [11,14]. Nickel phosphorus (NiP) alloy is a frequently considered material for the HER because of its unique features such as relatively higher activity than Ni toward the HER and its excellent properties in wear and corrosion [15]. Recently, we reported Ni-P-La alloy as a potential new catalyst for the HER that was characterized by Tafel slope, (b=-93.0 $mVdec^{-1}$), exchange current density (j_0=-181.0 μAcm^{-2}), and over potential at the current density of 250 mA cm^{-2}, (h_{250}=-139.0 mV). Although Ni-P-La is an active catalyst for the HER, its cost is high, which limits its use for industrial applications. In a previous study, we found that NiP composite coatings reinforced with co-deposited graphite carbon prepared by electrodeposition method provided benefits of good catalytic activity and stability for the HER; and therefore, this structure was anticipated to be a good candidate material for the HER [17]. Furthermore, the results of that study showed that the increase in the activity of the NiPC electrode was achieved by increases in both the surface roughness and the intrinsic activity (synergetic effect) [17]. In this paper, to further increase the catalytic activity of NiPC toward the HER, a three-dimensional NiPC (3D-NiPC) alloy was synthesized via a simple, cheap, and efficient method called the dynamic hydrogen bubble template (DHBT) [16], and its electrocatalytic activity was evaluated in alkaline solution.

2. Experimental

First, to prepare a three-dimensional copper substrate (3D-Cu), we used the DHBT method on a high pure Cu rod at the current density (j) of -100 mA cm^{-2} in a solution consisting of 0.6 M $CuSO_4$, 1.5 M H_2SO_4, and 1.0 M HCl. The electrodeposition of the NiPC alloy was performed in a three-step method under optimized conditions: first, a layer of Ni was deposited on the 3D-Cu from bath (i) including 0.83 M $NiSO_4$, 0.15 M Na_3Citrate, 0.15 M Na_2tartrate, at 25 °C, pH 4.6, and a current density of 16 $mAcm^{-2}$ for 30 min, followed by deposition of NiP from bath (ii) consisting of 1.0 M $NiSO_4$, 0.26 M H_3BO_3, and 0.3 M NaH_2PO_2, at the same temperature and pH, and a current density of 16 $mAcm^{-2}$ for 30 min. In the final step, (iii), eight gL^{-1} graphite powders (Aldrich®), with an average particle size of of 1 μm, was added to bath (ii), and electrodeposition was performed at a current density of 16 mA cm^{-2} and temperature of 80 °C for 3 h to finish preparing the 3D-NiPC alloy. For comparison, NiPC alloy (two-dimensional) was prepared by the method described previously in [16] on a copper disc surface. In all of the electrodeposition experiments, the counter electrode was a 25 cm^2 Pt plate, and all the electrochemical studies of the investigated alloys took place in a two-compartment Pyrex® glass cell consisting of a large surface area Pt plate electrode as the counter in the anodic compartment and a Hg/HgO/1M NaOH electrode linked to the main compartment of the cell (cathodic compartment) via a Luggin-Haber capillary as a reference. The Pyrex cell was equipped with a water jacket to control the temperature. A Biologic SP-150 potentiostat/galvanostat was used for all electrochemical analyses. All measurements were performed in purified 1 M NaOH solution in 298 K.

The steady-state polarization Tafel curves, electrochemical impedance spectroscopy (EIS), and cyclic voltammetry (CV) measurements were used to investigate the electrocatalytic activities of the prepared alloy. The kinetic parameters (i.e., Tafel slope b, exchange current density j_0, and overpotential at the current density of 250 mA cm^{-2}, h_{250}) were evaluated for the 3D-NiPC alloy using the linear least square (LLS) approximation method. Approximation of the EIS data was performed using ZView® software and

the modified complex nonlinear least square (CNLS) approximation method [17]. A one-CPE model was enough to explain the EIS data [18-20]. The field-emission scanning electron microscopy (FESEM) (ZIESS, SIGMA VP-500), energy dispersive spectrometry (EDS) and Brunauer, Emmett, and Teller (BET) (Microtrac Bel Corp, BELSORP) techniques were used to characterize the morphology of the investigated alloys.

3. Results and Discussion

The apparent activity of the 3D-NiPC alloy was studied by steady-state polarization Tafel curves. Typical curves obtained for the HER of the studied alloys in 1 M NaOH aqueous solutions are displayed in Fig. 1. The Tafel curve obtained for a 2D-NiPC alloy in the same experimental conditions is also presented in this figure for comparison.

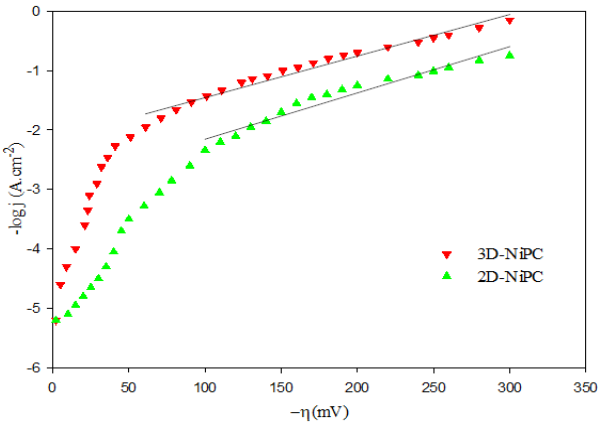

Fig.1. Steady-state polarization Tafel curves obtained on the studied alloys (3D-NiPC and 2D-NiPC) in 1 M NaOH at 298K.

As can be seen, two distinct regions of steady-state behavior were observed on the Tafel curve of the 3D-NiPC alloy. The linearity of the Tafel plot at negative potentials indicates that the HER proceeds via reactions of Volmer and Heyrovsky (the Volmer-Heyrovsky mechanism, the influence of the Tafel reaction is negligible) [13]. The kinetic parameters obtained from steady-state Tafel curves at high overpotentials are presented in Table 1.

Table 1. The HER kinetic parameters for 2D-NiPC and 3D-NiPC alloys obtained from polarization Tafel curves in 1M NaOH at 298 K.

Alloy	-b (mV dec^{-1})	-j_0 (×10^{-3} A cm^{-2})	-η_{250} (mV)
2D-NiPC	112.5±0.8	1.30.1±	360.62.6±
3D-NiPC	118.5±1.6	7.0±0.2	173.3±1.4

Therefore, the 3D-NiPC alloy was characterized by exchange current density: j_0 = 7.0 ±0.2 (×10^{-3} A cm^{-2}), the Tafel slope: b=118.5 ±1.6 mV dec^{-1}, and a low overpotential at sufficiently large current density (e.g., overpotential at 250 mAcm^{-2}; η_{250}) 173.3±1.4 mV. From comparison with two-dimensional NiPC Tafel parameters in Table 1, it is seen that three-dimensional structures remarkably increases the hydrogen evolution activity as shown in Fig. 1; the η_{250} value for 3D-NiPC is 173.3 mV, which is much smaller than the 2D-NiPC alloy (η_{250}=360.6 mV). However, EIS studies were performed to obtain more precise quantitative kinetic information about the activity. The EIS experimental data were collected for the HER on the 3D-NiPC alloy in 1M NaOH at 298 K in the potential range corresponding to the linear part of the Tafel plots. Typical complex-plane plots at various overpotentials are presented in Fig. 2.

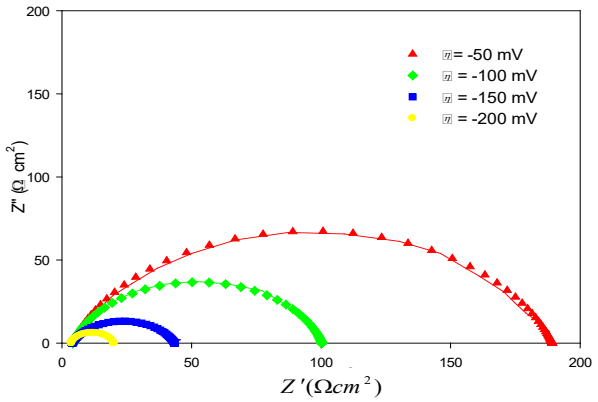

Fig.2. Complex-plane plots for 3D-NiPC alloy at various overpotentials (η) and 298 K. Symbols indicate experimental results and solid lines approximate data obtained using one-CPE model and CNLS.

The entire complex plane plots showed one semicircle (Fig. 2) that varied with the potential and was attributed to the charge transfer resistance of the HER. A one-CPE model containing a parallel R-constant phase element (CPE) in series with uncompensated resistance, due to the cell and electrodes configuration, has been used to approximate the EIS data. The impedance of the CPE is described by $Z_{CPE}= 1/T (J\omega)^{\varphi}$ and was used to simulate the depression of the semicircle in the complex plane plots at various overpotentials. In this model, T is a capacitive parameter related to the average double-layer capacitance (C_{dl}), $T = C_{dl}^{\varphi} (R_S^{-1} + R_{ct}^{-1})^{1-\varphi}$ [21,22] and other parameters are defined as $J = (-1)^{1/2}$, solution resistance (R_s), charge transfer resistance (R_{ct}), angular frequency ($\omega = 2\pi f$), and the φ parameter, which is related to the CPE model (the value of φ changes between zero to one) and is equal to one for complete smooth electrode, for $\varphi = 1$, $T = C_{dl}$. The EIS experimental data were approximated and analyzed using the one-CPE model and CNLS method from which kinetic parameters such as C_{dl}, R_{ct}, and roughness factor (R_f) were extracted as shown in Table 2. The roughness factor was estimated by equation (1) [23]:

$$R_f = C_{dl} / (20\ \mu Fcm^{-2}) \quad (1)$$

Table 2. HER kinetic parameters for 3D-NiPC alloy obtained from the EIS experiments in 1 M NaOH at η=-100 mV.

Catalyst	R_s(Ωcm²)	R_{ct} (Ωcm²)	C_{dl} (Fcm^{-2})	φ[b]	R_f
2D-NiPC	1.11	151.1	0.025	0.81-0.88	1250
3D-NiPC	0.99	100.6	0.071	0.71-0.82	3550

[a]Total resistance

[b]Dispersion parameter related to CPE model

As seen in Table 2, a roughness factor of 1250 and 3550 was obtained for 2D-NiPC and 3D-NiPC alloys, respectively. The larger roughness for 3D-NiPC alloy agrees with its higher surface area that originated from its three-dimensional structure. The three-dimensionality of 3D-NiPC enhances its active sites for the H_2 evolution reaction, as shown in Table 2. The charge transfer resistance of this structure is smaller, at about 50 Ω cm², than two-dimensional NiPC.

Apart from the catalytic activity, the stability of the investigated alloy is another important property for the HER. Therefore, the long-term stability of the three-dimensional NiPC alloy was investigated in 1M NaOH at two different overpotentials, η_{100} and η_{250}, which relate to current densities of 100 and 250 mAcm^{-2}, respectively. In Fig. 3, the time-dependent current density curves of the 3D-NiPC alloy tested for 100 hours at two constant overpotentials (η_{100} and η_{250}) are shown. These experiments showed that the 3D-NiPC alloy's responses were physically, chemically, and electrochemically stable for a relatively long time (100 h) in the HER in 1 M NaOH at 298 K.

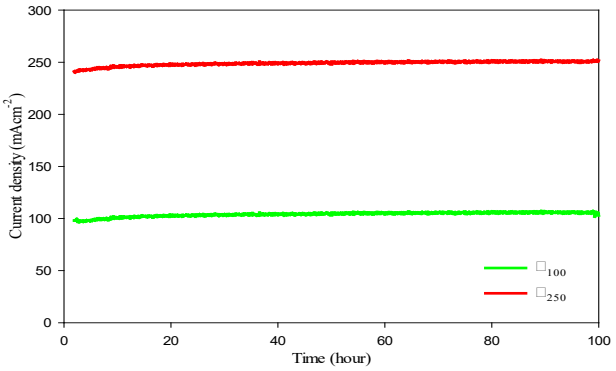

Fig. 3. Constant potential curves obtained for 3D-NiPC alloy in 1 M NaOH at 298 K.

The composition, physical stability, and activity for the HER of the 3D-NiPC alloy depend on various parameters such as current density, the concentration of the chemical reagents in the bath, and steps of layers deposition. The electrodeposition of 3D-NiPC was prepared in "three steps. First, a layer of Ni was

deposited on 3D-Cu from bath (i), including 0.83 M" $NiSO_4$, 0.15 M Na_3Citrate, 0.15 M Na_2tartrate, at 25 °C, pH 4.6, and a current density of 16 $mAcm^{-2}$ for 30 min, followed by deposition of NiP from bath (ii) consisted of 1.0 M $NiSO_4$, 0.26 M H_3BO_3, and 0.3 M NaH_2PO_2 at the same temperature and pH, and a current density of 16 $mAcm^{-2}$ for 30 min. In the final step (iii), eight gL^{-1} graphite powders (Aldrich®) with a 1 µm average particle size, were added to bath (ii), and electrodeposition was performed at a current density of 16 mA cm^{-2} and temperature of 80 °C for 3 h to prepare the 3D-NiPC alloy. The SEM images of the 2D- (a) and 3D-NiPC (b) alloys are shown in Fig. 4. As can be observed in Fig. 4b, there are numerous pores and fine ramified walls on the surface of the 3D-NiPC alloy, indicating a large surface area available for the HER.

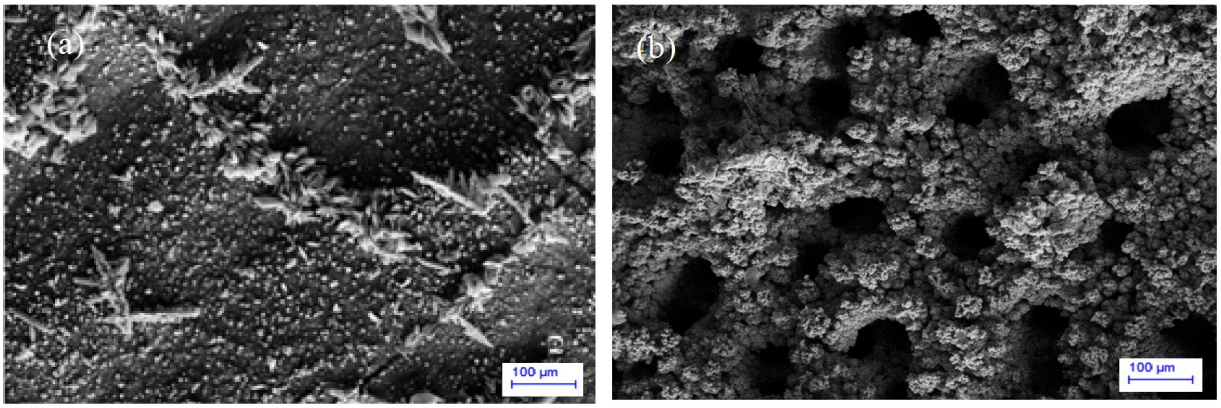

Fig.4. SEM images of the synthesized 2D- (a) and 3D-NiPC (b) alloys.

Furthermore, this construction probably accounts for the high physical stability, electrochemical activity, and large real surface area of the electrode. The chemical composition of the electrodeposits prepared under optimized conditions was determined by EDX analysis to be $Ni_{71}P_{26}C_3$. Also, the BET measurements were performed and gave a specific surface area of 1.012 and 8.112 m^2gr^{-1} for 2D and 3D-NiPC alloys, respectively. Therefore, the 3D-NiPC alloy shows a larger specific surface area, which is in good agreement with Fig. 4.

4. Conclusion

In this work, a large surface area three-dimensional structure of NiPC alloy (3D-NiPC) was prepared by a simple, cheap, and efficient method called dynamic hydrogen bubble template (DHBT). The electrocatalytic behavior of this structure was studied quantitatively by potential polarization Tafel curves and the EIS methods for the first time. The 3D-NiPC alloy showed high electrocatalytic activity toward the HER as revealed by merit parameters like the Tafel slope (b=-118.5±1.6 $mVdec^{-1}$) and overpotential at 250 $mAcm^{-2}$ (h_{250}=173.3±1.4) obtained from linear regression analysis of the potential polarization curves. The C_{dl} approximated by the EIS data allowed the evaluation of the R_f of the electrode (R_f=3550). The 3D-NiPC alloy was physically, chemically, and electrochemically stables for a relatively long time HER (100 h) in 1 M NaOH at 298 K.

References

[1] Nikolic V.M., Maslovara S.L., Tasic G.S., Brdaric T.P., Lausevic P.Z. and Radak B.B., „Kinetics of hydrogen evolution reaction in alkaline electrolysis on a Ni cathode in the presence of Ni–Co–Mo based ionic activators“, Applied Catalysis B, 2015, 179: 88-94.

[2] Yan X. , Huang S. , Yang F., Sun S., Zhang G., Jiang B., Zhang B., Che S., Yang W. and Li Y., „Eni

hanced catalytic hydrogen evolution reaction performance of highly dispersed Ni2P nanoparticles supported by P-doped porous carbon“, Colloids and Surfaces A, 2021, 616: 126308.

[3] Aqeel Ashraf M., Li C., Thai Pham B. and Zhang D. , „Electrodeposition of Ni–Fe–Mn ternary nanosheets as affordable and efficient electrocatalyst for both hydrogen and oxygen evolution reactions“, Int. J. Hydrogen Energy, 2020, 45: 24670-24683.

[4] Elrouby M., Sadek M., Mohran H.S. and Abdel Lateef H.M., „A highly stable and efficient electroffi deposited flowered like structure Ni–Co alloy on steel substrate for electrocatalytic hydrogen evolution reaction in HCl solution“, J. Materials Research and Technology, 2020, 9: 13706-13717.

[5] Yang W. and Chen S., „Recent progress in electrode fabrication for electrocatalytic hydrogen evolution reaction: A mini review“, Chemical Engineering J., 2020, 393: 124726.

[6] Shervedani R.K. and Madram A.R., „Kinetics of hydrogen evolution reaction on nanocrystalline electrodeposited $Ni_{62}Fe_{35}C_3$ cathode in alkaline solution by electrochemical impedance spectroscopy“, Electrochimica Acta, 2007, 53: 426-433.

[7] Safizadeh F., Ghali E. and Houlachi G., „ElecS trocatalysis developments for hydrogen evolution reaction in alkaline solutions- A Review“, Int. J. Hydrogen Energy, 2015, 40: 256-274.

[8] Meguro S., Sasaki T., Katagiri H., Habazaki H., Kawashima A., Sasaki T., Asami K. and Hashimoto K., „Electrodeposited Ni-Fe-C Cathodes for Hyo drogen Evolution“, J. Electrochemical Society, 2000, 47: 3003.

[9] Divisek J., Schmitz H. and Steffen B., „Electroi catalyst materials for hydrogen evolution“, Electrom chimica Acta, 1994, 39: 1723-1731.

[10] Losiewicz B., Budniok A., Rowinski E., Lagiewka E. and Lasia A., „Effect of heat-treatment on the mechanism and kinetics of the hydrogen evolution reaction on Ni-P+TiO_2+Ti electrodes“, J. Applied Electrochemistrty, 2004, 34: 507-516.

[11] Sun T., Cao J., Dong J., Du H., Zhang H., Chen J. and Xu L., „Ordered mesoporous Ni-Co alloys for highly efficient electrocatalytic hydrogen evolution reaction“, 2017, 42: 6637-6645.

[12] Anaam H., Ali A.S., Jedidi A., Anjum D.H., Cavallo L. and Takanabe K., „Kinetics on NiZn bimetallic catalysts for hydrogen evolution via selective dehydrogenation of methylcyclohexane to toluene“, ACS Catalysis, 2017, 7: 15921600.

[13] Shervedani R.K. and Lasia A., „Studies of the hydrogen evolution reaction on Ni-P electrodes“, J. Electrochemical Society, 1997, 144: 511-519.

[14] da Silva M.G.S., Leite C.M., Cordeiro M.L., Mastelaro V.R. and Leite E.R., „One-step synthesis of nickel sulfides and their electrocatalytic activities for hydrogen evolution reaction: a case study of crystalline h-NiS and oNi_9S_8 nanoparticles“, ACS Applied Energy Materials, 2020, 3: 9498-9503.

[15] Li Z.P., Shang J.P., Su C.N., Zhang S.B., Wu M.X. and Guo Y., „Preparation of amorphous NiP-based catalysts for hydrogen evolution reactions, Journal of Fuel Chemistry and Technology“, 2018, 46: 473-478.

[16] Vesztergom S., Dutta A., Rahaman M., Kiran K., Montiel I.Z. and Broekmann P., „Hydrogen bubble templated metal foams as efficient catalysts of CO_2 electroreduction“, Chemical Catalysis Chemistry, 2021, 13: 10391058.

[17] Macdonald J.R., Schoonman J. and Lehner A.P., „Applicability and power of complex nonlinear least squares for the analysis of impedance and admittance data“, J. Electroanalytical Chemistry, 1982, 131: 77.

[18] Rausch S. and Wendt H., „Morphology and utilization of smooth hydrogen-evolving raney nickel cathode coatings and porous sintered-nickel cathodes“, J. Electrochemical Society, 1996, 143: 2852.

[19] Chen L. and Lasia A., „Ni-Al powder electrocatA alyst for hydrogen evolution: effect of heat-treatment on morphology, composition, and kinetics“, J. Electrochemical Society, 1993, 140: 2464.

[20] (a) Los P., Lasia A., Menard H. and L. Brossard, „Impedance studies of porous lanthar num-phosphate-bonded nickel electrodes in concentrated sodium hydroxide solution“, J. Electroanu alytical Chemistry, 1993, 360: 101.

(b) Jurczakowski R., Hitz C. and Lasia A., „Impedu ance of porous gold electrodes in the presence of electroactive species“, J. Electroanalytical Chemise try, 2005, 582: 85.

[21] Brug G.J., van der Eden A.L.G., Rehbach M.S. and Sluyters J.H., „The analysis of electrode imy pedances complicated by the presence of a constant phase element“, J. Electroanalytical Chemistry, 1984, 176: 275-295.

[22] Brug G.J., Rehbach M.S., Sluyters J.H. and

Hemelin A., „The kinetics of the reduction of protons at polycrystalline and monocrystalline gold electrodes“, J.Electroanalytical Chemistry and Interfacial Electrochemistry, 1984, 176: 275-295.

[23] Lasia A., Rami A., „Kinetics of hydrogen evolution on nickel electrodes“, J. Electroanalytical Chemistry, 1990, 294: 123-141.